Int. J. Electrochem. Sci., 14 **(2019)** 11358 – 11366, doi: 10.20964/2019.12.45

International Journal of
ELECTROCHEMICAL
SCIENCE
www.electrochemsci.org

A Facile Synthesis of Cu-MnO/CNF by Electrospinning Method and Its Electrochemical Performance for Supercapacitor Application

Chunyong Zhang[1,2,], Lei Su[1,2], Linna Huang[1,2], Jiehong Cheng[2,3,*], Jianning Li[1,2], Hengfei Qin[2,3]*

[1] Jiangsu Key Laboratory of Precious Metal Chemistry and Technology, Jiangsu University of Technology, Changzhou, 213001, China
[2] School of Chemistry and Environmental Engineering, Jiangsu University of Technology, Changzhou, 213001, China
[3] Jiangsu Province Key Laboratory of E-Waste Recycling, Jiangsu University of Technology, Changzhou, 213001, China
Chunyong Zhang, Lei Su contributed equally to this work and should be considered as co-first authors
[*]E-mail: zhangcy@jsut.edu.cn, cjh@jsut.edu.cn

Received: 25 July 2019 / *Accepted:* 20 September 2019 / *Published:* 29 October 2019

The carbon nanofiber composite containing Cu and MnO was fabricated by electrospinning method. The precursor solution was prepared by mixing Cupric Acetate Monohydrate, Manganous acetate, N,N-dimethylformamide (DMF) and polyacrylonitrile in a certain proportion. Then the material of Cu-MnO/CNF with higher capacitance was prepared by electrostatic spinning at 15 kV and high temperature heat treatment. The Cu-MnO/CNF was characterized by scanning electron microscopy (SEM) and X-Ray diffraction (XRD). It's clear from the results that, carbon nanofiber had overlaped by metal oxides and metals, at the same time, the $Cu(OAc)_2$ was converted to Cu and the MnACAC was turned into MnO after thermal treatment. Through a series of electrochemical tests, it showed the Cu-MnO/CNF has excellent electrochemical performance and indicated its potential advantages for supercapacitors. The results indicated the specific capacitance of the Cu-MnO/CNF displayed a larger specific capacitance of 581 F/g than the electrical capacity of Cu-CuO/CNF and MnO-$Mn(OH)_2$/CNF.

Keywords: Supercapacitor; Carbon Nanofiber; Electrospinning; Specific Capacitance

1. INTRODUCTION

As the new energy storage devices developed, the emergence of supercapacitors has attracted well attention[1]. Excellent characteristics such as large capacity, long cycle life, high charge and discharge efficiency, and high power density make supercapacitors have good application prospects[2-5]. However, the preparation of electrode materials is a key point affecting the performance of supercapacitors[6]. Based on the electrospinning technology, this paper focuses on the research of

electrospinning carbon nanofiber (CNF) composites in electroanalytical chemistry. Electrospinning is a new technology that can produce nanometer-diameter filaments with a minimum diameter of 1 nm. It is the only method capable of directly and continuously preparing polymer nanofibers. It has been widely used in the field of nanofiber preparation. The application is considered to be one of the simplest and most effective methods, and different nanofibers have been successfully prepared by this method. Electrospinning technology is simple, convenient, inexpensive, and environmentally friendly[7]. At present, carbon black is the main carrier of electrode materials, and carbon nanomaterials are continuously studied because of their conductive and thermal conductivity. As a new kind of carbon materials, carbon nanofibers are new materials with good physical and chemical properties[8-11]. As the electrode material of supercapacitor, Cu has the disadvantages of being polluted and not uniformly dispersed in CNF[12]. It is the research direction of supercapacitors to load new metal oxides[13] on CNF to prepare electrodes with large capacitance, long life and low pollution.

In this work, MnACAC was used as a precursor of MnO. Among many inorganic functional materials, manganese oxide materials are becoming more and more popular with their own safety innocuity, high specific capacity and low price, and the electrode materials prepared by it have high specific capacity and high stability. The Manganese acetylacetonate was added to the electrospun precursor solution, which significantly improves the electrochemical performance of the electrode[14].

Up to now, there are few reports about MnACAC and $Cu(OAc)_2$ used as a precursor for supercapacitor electrodes. Its high specific volume rate makes it suitable for electrode materials of capacitors. This work prepared Cu-MnO/CNF, improved the uneven distribution of Cu in CNF and improved the electrochemical performance.

2. EXPERIMENTAL

2.1. Chemicals

Potassium hydroxide (KOH), solvent N,N-dimethylformamide (DMF), Isopropanol and Ethanol (C_2H_5OH) were obtained from Sinopharm Chemical Reagent Co., Ltd. Polytetrafluoroethylene (5 μm), Acetylene black, $Cu(OAc)_2$ salt (≥98%), MnACAC (≥97%) and PAN (Mw =150,000) were purchased from Aladdin.

2.1 Preparation of the precursor solution

Fig. 1 shows the schematic of electrospinning. The precursor solution of $Cu(OAc)_2$/PAN was consisted of 1.3 g PAN, 12 mL DMF and 1.3 g $Cu(OAc)_2$. The precursor solution of MnACAC/PAN referred to the previous step. Preparation of $Cu(OAc)_2$-MnACAC/PAN-10 wt% of PAN was prepared by dissolving the PAN in DMF by stirring for 2 h to form uniform aqueous, $Cu(OAc)_2$ (8 wt%) and MnACAC (8 wt%) were mixed in order to get the electrospinning liquid solved with magnetic stirring for 6 h at room temperature. The collected optimal conditions for electrospun nanofibers were a constant feed rate of 1 mL/h under the positive voltage of 15 kV and a length of 15 cm between the spinneret and the fiber collector.

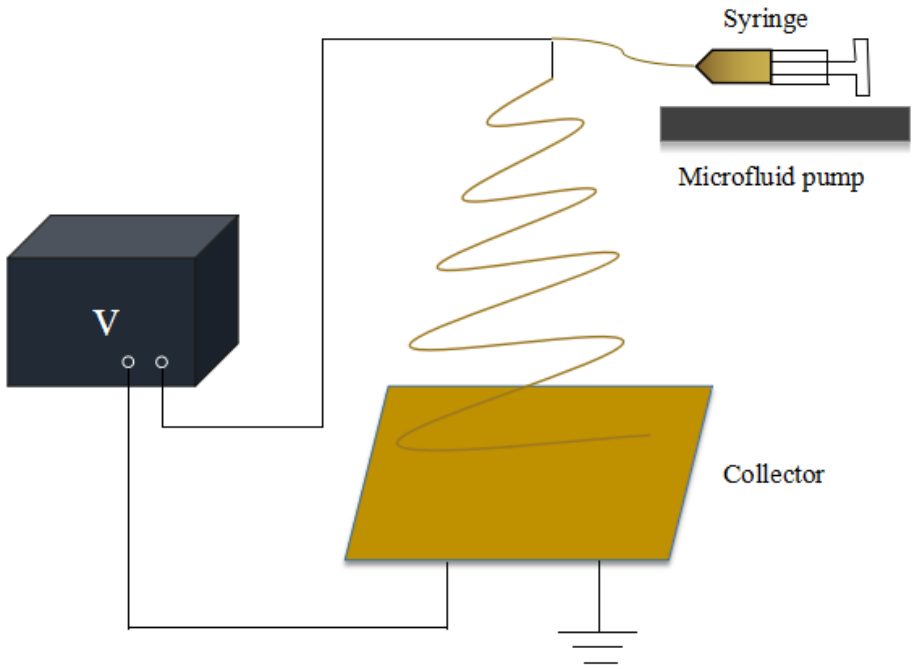

Figure 1. Schematic diagram of electrospinning

2.2 Fabrication of Cu-CuO/CNF, MnO-Mn(OH)$_2$/CNF, Cu-MnO/CNF

The collected nanofiber films of Cu(OAc)$_2$/PAN oxidized at 250 °C in air at a rate of 5 °C/min and dwell time 2 h. The films were completely carbonized under temp 700 °C in N_2 at a rate of 3 °C min^{-1}, dwell time of 2 h. The collected nanofiber films of MnACAC/PAN oxidized at 260 °C in air at a rate of 3 °C/min and dwell time 2 h. The films were then fully carbonized at 850 °C in N_2 (at a rate of 5 °C/min, dwell time of 2 h at 550 °C, at a rate of 2 °C/min, dwell time of 2 h at 850 °C). The collected nanofiber films of Cu(OAc)$_2$- MnACAC/PAN oxidizedat 290 °C in air at a rate of 5 °C/min and dwell time 2 h. The films were then fully carbonized at 850 °C in N_2 (at a rate of 5 °C/min, dwell time of 2 h at 600 °C, at a rate of 5 °C/min, dwell time of 2 h at 850 °C).

2.3 Characterization and electrochemical testing

The surface morphology of nanofibers was observed by scanning electron microscopy (SEM, Hitachi S-3400N). The substance contained in the nanofibers was determined by high-resolution transmission electron microscopy (XRD, PW3040/60, PANalytical B.V, the scanning range of 2θ is 5-90°). The electrochemical analysis of nanofibers was measured by electrochemical workstation (CHI760E). The electrode system was a three-electrode system, with the nickel foam as the working electrodes, platinum gauze electrode and saturated calomel electrode were used as pair electrodes and reference electrodes respectively. The working electrode of the nickel foam was prepared by mixing the sample, PVDF and acetylene black at a mass ratio of 8:1:1, adding 2 mL of isopropyl alcohol as a dispersing agent, uniformly stirring and coating on the previously prepared nickel foamed, and the application area was 1.0 cm×1.0 cm and drying for 12 hours in a vacuum drying box of 60 °C. The experiments were carried out in 6 M KOH electrolyte at room temperature. The cyclic voltammograms

was performed by varying the scan rate from 5 to 60 mV/s. The galvanostatic charge-discharge curves were carried out in a range from -0.12 to 0.20 V and specific currents of 0.5 A/g, 1 A/g, 2 A/g, 3 A/g and 4 A/g were applied. The specific capacitance was calculated based on the following equation:

$$C_s = \frac{\int IdV}{2m \cdot v \cdot \Delta V}$$

which C_s was the specific capacitance (F/g), I was the current (A), m means the quality of electrode material (g), v was the sweep speed (V/s) and ΔV was the range of voltage (V). The electrochemical impedance spectroscopy measured under the range from100 kHz to 0.01 Hz.

3. RESULTS AND DISCUSSION

Due to high specific capacitance and excellent chemical stability, Manganic acetylacetonate suitable for electrode materials of capacitors. Non-precious metal-carbon nanofiber composites are widely used in supercapacitors, such as MnO_2/PPy@CNF (manganese dioxide/PPy/carbon nanofiber), Mn@CNF (manganese acetylacetonate@carbon nanofiber), CNF/G (carbon nanofiber/graphene), ZnO/CNFs (zinc oxide/carbon nanofiber), MnO_x@CNF (manganese oxide@carbon nanofibers), NiO_x/CNF (nickel oxide/carbon nanofibers). And Table 1 summarizes the capacitance properties of the carbon nanofibers loaded different metals.

Table 1. Non-noble metal loaded on carbon nanofibers for capacitance testing

Electrode Material	Electrochemical testing equipment	Test Solutions	Specific power/Mass activity	Reference
MnO_2/PPy@CNF	CHI660B	2 M KCl	705 F/g	[15]
Mn@CNF	/	0.25 M LiTFSI	200 F/g	[16]
CNF/G	CHI660D	6 M KOH	250 F/g	[17]
ZnO/CNFs	/	6 M KOH	216 F/g	[18]
MnO_x@CNF	CHI660D	6 M KOH	335 F/g	[19]
CNT/CNF	Gamry Reference 600	1 M KOH	241 F/g	[20]
Cu-MnO/CNF	CHI760E	6 M KOH	581 F/g	This work

Fig. 2 shows Scanning Electron Microscope photos of Cu-CuO/CNF, MnO-$Mn(OH)_2$/CNF and Cu-MnO/CNF electrodes. It can be observed that the Cu nanoparticles were loaded on carbon nanotubes with the form of sphere in Fig. 2A with the addition of copper salts. The Cu nanoparticles loaded on the surface of CNF were dispersive and not dense. As can be seen from Fig. 2B, the Mn nanoparticles loaded on CNF display blocky structure. The Mn nanoparticles distribute uniformity and

not in identical size. According to Fig. 2C that Mn and Cu nanoparticles are highly dispersed on the surface of CNF. We can clearly observe that the nanoparticles distribute evenly and arrange neatly.

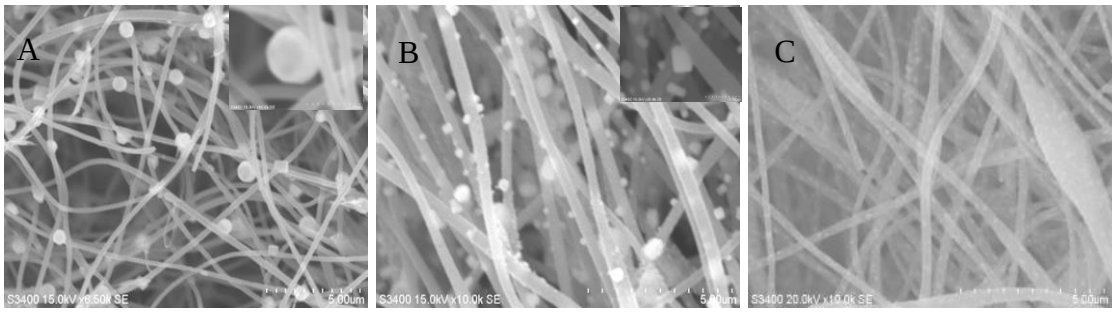

Figure 2. SEM photos of (A) Cu-CuO/CNF, (B) MnO-$Mn(OH)_2$/CNF, (C) Cu-MnO/CNF

The diffractograms of the X-ray diffraction patterns of Cu-CuO/CNF, MnO-$Mn(OH)_2$/CNF and Cu-MnO/CNF nanocomposites can be observed in Fig. 3. XRD patterns of as-prepared electrodes were recorded on D/MAX-2500PC (Rigaku Miniflex II) Instrument run by Cu Kα radiation (λ = 1.5406 Å) with the scattered angle range of 5° to 90°, operating at 40 kV and 40 mA. According to the Cu nanoparticles loaded on the surface of CNF in Fig. 3A, the vital diffraction peak of Cu around 2θ = 43.3°, 50.4°, 74.1°, 89.9° corresponding to Cu (112), (200), (220), (331). The electrode materials with better capacitance can be prepared by loading Cu on CNF to increase its conductivity[21]. However, there are CuO impurities, the diffraction peaks at 35.4°, 38.4° corresponding to CuO (11-1) and (200) crystal planes. The MnO-$Mn(OH)_2$/CNF diffractogram shows in Fig. 3B. There are six peaks around 2θ = 35.2°, 40.8°, 58.8°, 70.4°, 74.0°, 89.9° relating to MnO(111), (200), (220), (331), (222), (400). The MnO loaded on CNF improves the power storage capacity and has good cycling stability[22-23]. But there are $Mn(OH)_2$ impurities, the diffraction peaks at 50.7° assigned to the (102) plane. From the Fig. 3C, the substance removed the impurity CuO and MnO-$Mn(OH)_2$, its storage and recycling properties will be further improved.

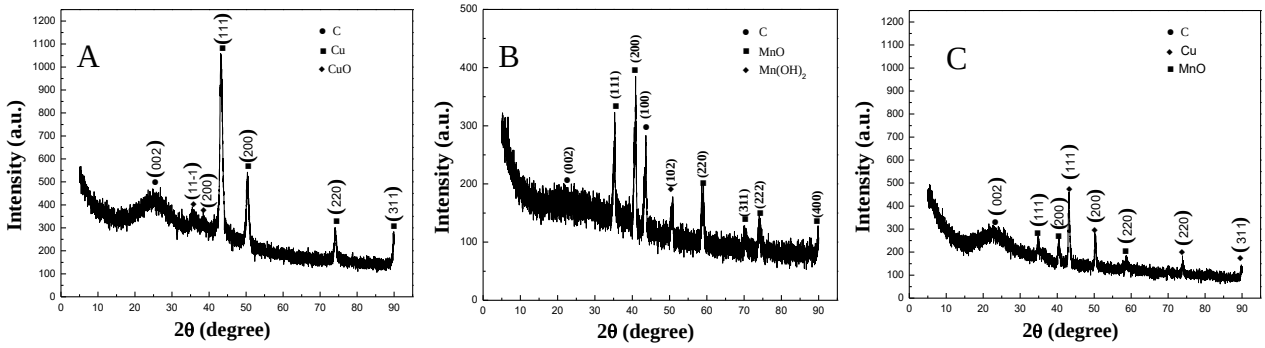

Figure 3. XRD patterns of (A) Cu-CuO/CNF, (B) MnO-$Mn(OH)_2$/CNF, (C) Cu-MnO/CNF

Fig. 4 shows the cyclic voltammetry (CVs) of the Cu-CuO/CNF, MnO-$Mn(OH)_2$/CNF and Cu-MnO/CNF electrodes with different scan rates in 6 M KOH. As can be seen in the following images, the cyclic voltammetry curve forms a pattern similar to a rectangle[24]. Cyclic volt-ampere curve of the Cu-MnO-CNF electrodes at the scan rate of 5 mV/s presented a better rectangular shape than that

of the Cu-CuO/CNF and MnO-Mn(OH)$_2$/CNF electrodes in Fig. 4A, which could be due to the absence of other impurities, the Mn and Cu nanoparticles are uniformly loaded onto the CNF, the area of contact with the electrolyte is increasing and thus reduce the resistivity of the electrode in the electrolyte. Among the four electrodes, Cu-MnO/CNF has the largest area of the rectangle, which indicates that Cu-MnO/CNF has higher capacitance and better cycle stability. In the cyclic voltammetry curves, because of the fast and reversible surface redox reactions of the electrolyte ion in the interface of electrodes, there is no obvious redox peak[25].

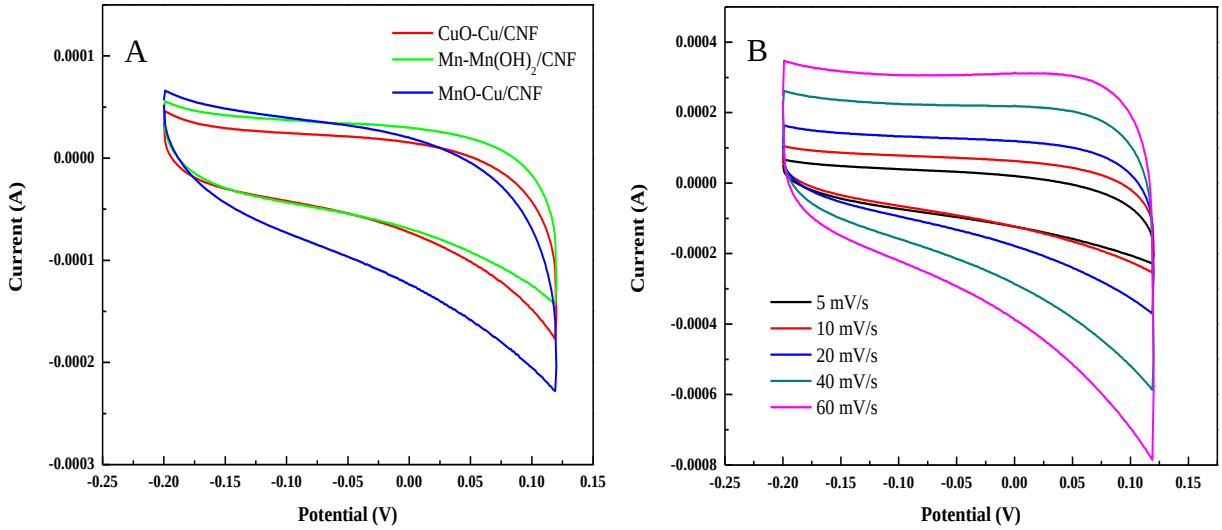

Figure 4. The cyclic voltammograms of (A) Cu-CuO/CNF, MnO-Mn(OH)$_2$/CNF, and Cu-MnO/CNF in 6 M KOH at 5 mV/s, (B) Cu-MnO/CNF in 6 M KOH at different scan rates at room temperature

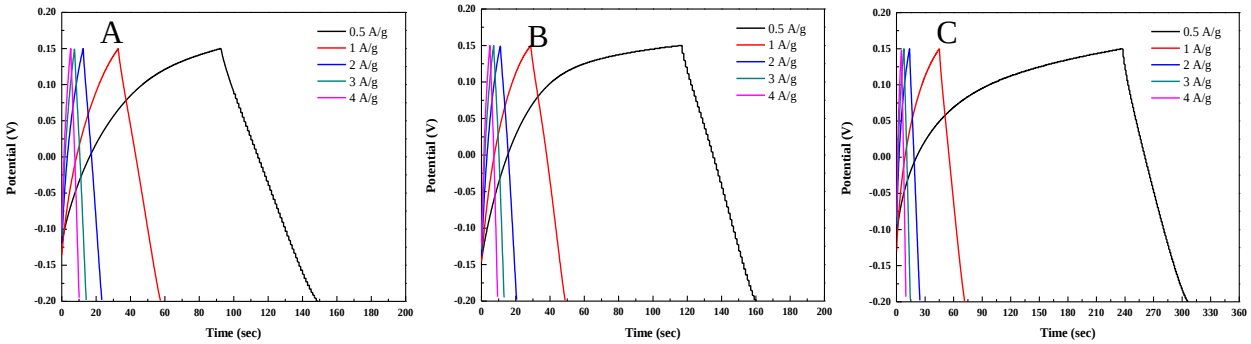

Figure 5. the galvanostatic charge-discharge curves of (A) MnO-Mn(OH)$_2$/CNF, (B) Cu-CuO/CNF, (C) Cu-MnO/CNF in 6 M KOH with different current densities

Fig. 5 shows the Constant Current Charge-Discharge Curve of these four electrodes at different current densities in 6 M KOH. It can be seen from the figures that the current density increases once from right to left, voltage is not linear to time. It is shown that the capacitance mainly comes from the pseudo capacitance produced by Cu-MnO/CNF electrode material, which has the longest charging and discharging time, indicating that the electrode material with MnO and Cu nanoparticles has the best capacitance.

Fig. 6 shows the specific capacitance (Csp) of Cu-CuO/CNF, MnO-Mn(OH)$_2$/CNF and Cu-MnO/CNF Electrodes at Different Scanning Rates 6 M KOH. It can be clearly seen that the specific

capacitance of the Cu-MnO/CNF electrode material is greater than other three materials, which is consistent with the results of the cyclic voltammetry curve. The value of specific capacitance decreases with the increase of scanning rate. According to the trend of the curve, the maximum specific capacitance of the Cu-MnO/CNF electrode material is 581 F/g.

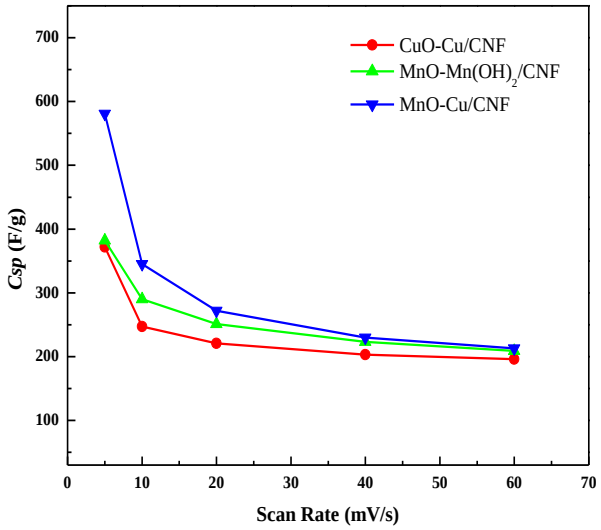

Figure 6. the specific capacitance (Csp) of Cu-CuO/CNF, MnO-Mn(OH)2/CNF and Cu-MnO/CNF in 6 M KOH with different scan rates

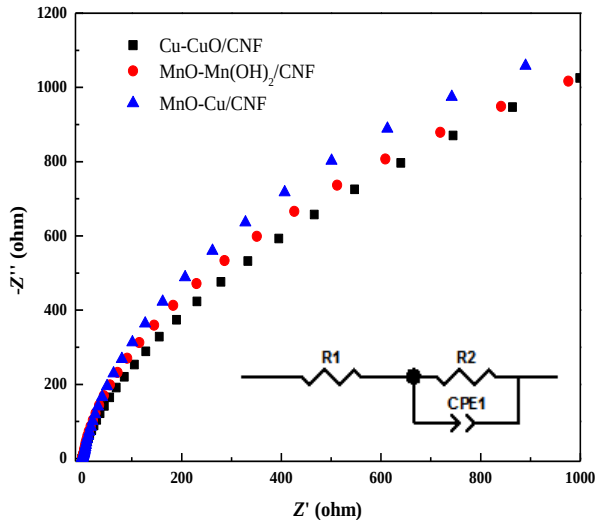

Figure 7. the electrochemical impedance spectroscopy of Cu-CuO/CNF, MnO-Mn(OH)2/CNF and Cu-MnO/CNF electrodes in 6 M KOH

Fig. 7 shows the electrochemical impedance spectroscopy of Cu-CuO/CNF, MnO-Mn(OH)2/CNF and Cu-MnO/CNF electrodes in 6 M KOH. The small arc is under high frequency region and the straight segment is in low frequency region. In theory, a straight line almost vertical is the ideal capacitor[26]. According to the picture, in the low frequency region, the impedance arc radius order is Cu-MnO/CNF>MnO-Mn(OH)2/CNF>Cu-CuO/CNF, as mentioned above the Cu-MnO/CNF material has good capacitance characteristics, diffusions well. In the high frequency region, the radius of the arc reflects the electrochemical process of the electrode material and the structural resistance. However, for capacitors with carbon nanotube-based electrodes, there is no semicircle.This indicates it

that there is no such contact resistance. The results show that the carbon nanotubes have close contact with the collector and provide an excellent network with well conducted.

4. CONCLUSION

In this work, the metals and metal oxide are successfully loaded on the surface of CNF and carbonized by electrospinning. In the carbonization treatment, metals and metal oxide were formed by carbonization reduction. The Cu and MnO were well-proportioned distributed on the CNF and arranged neatly. The electrochemical activity and stability of Cu-MnO/CNF electrodes are higher than those of Cu-CuO/CNF, MnO-$Mn(OH)_2$/CNF electrodes, and their specific capacitance increased from 213 F/g to 581 F/g. The charge and discharge time of Cu-MnO/CNF was the longest. The side reflects the Cu-MnO/CNF has a good conductive property and shows better capacitance characteristics. This is consistent with the calculated specific capacitance.

ACKNOWLEDGEMENT
This work was supported by Postgraduate Research&Practice Innovation Program of Jiangsu Province (20820111964-SJCX19-0754) and (20820111950-SJCX19-0740), National Natural Science Foundation of China (grant no. 31800495), Natural Science Foundation of Jiangsu Province (grant no. BK20181040).

References

1. S. Park and S. Kim, *Electrochimica Acta*, 89 (2013) 516.
2. Z. Jin, M. U. Weifang, C. Zhang, H. E. Tieshi, Q. Zhang, J. Hou and K. Cai, *Electrochimica Acta*, 59 (2012) 100.
3. C. John, L. Celine, T. Pierre-Louis, S. Patrice and G. Yury, *Science*, 328 (2010) 480.
4. Q. Sun, *International Journal of Electrochemical Science*, 1 (2019) 14.
5. W. Yinwei, *International Journal of Electrochemical Science*, 618 (2019) 624.
6. Z. Yong, F. Hui, X. Wu, L. Wang, A. Zhang, T. Xia, H. Dong, X. Li and L. Zhang, *International Journal of Hydrogen Energy*, 34 (2009) 4889.
7. P. Raghavan, D. H. Lim, J. H. Ahn, C. Nah, D. C. Sherrington, H. S. Ryu and H. J. Ahn, *Reactive & Functional Polymers*, 72 (2012) 915.
8. G. S. Chai, S. B. Yoon and J. S. Yu, *Carbon*, 43 (2005) 3028.
9. X. Chen, Y. Zhang, X. P. Gao, G. L. Pan, X. Y. Jiang, J. Q. Qu, F. Wu, J. Yan and D. Y. Song, *International Journal of Hydrogen Energy*, 29 (2004) 743.
10. Y. H. Hsu, C. C. Lai, C. L. Ho and C. T. Lo, *Electrochimica Acta*, 127 (2014) 369.
11. N. M. Rodriguez, *Journal of Materials Research*, 8 (1993) 3233.
12. A. Shin, Y. I. Kim, S. H. Ko and J. H. Han, *Journal of Alloys & Compounds*, 737 (2017).
13. J. P. Zheng and T. R. Jow, *Mrs Proceedings*, 393 (1995) L6.
14. S. Hassan, M. Suzuki, S. Mori and A. A. El-Moneim, *Journal of Power Sources*, 249 (2014) 21.
15. K. Karthikeyan, D. Kalpana and N. G. Renganathan, *Ionics*, 15 (2009) 107.
16. X. Liu, M. N. Marlow, S. J. Cooper, B. Song, X. Chen, N. P. Brandon and B. Wu, *Journal of Power Sources*, 384 (2018) 264.
17. CHUANG, ChihMing, HUANG, ChengWei, H. Teng, TING and JyhMing, *Composites Science & Technology*, 72 (2012) 1524.
18. S. Shi, X. Zhuang, B. Cheng and X. Wang, *Journal of Materials Chemistry A*, 1 (2013) 13779.

19. H. C. Hsu, C. H. Wang, Y. C. Chang, J. H. Hu, B. Y. Yao and C. Y. Lin, *Journal of Physics & Chemistry of Solids*, 85 (2015) 62.
20. R. D. Noce, S. Eugénio, M. Boudard, L. Rapenne, T. M. Silva, M. J. Carmezim, S. Donne and M. F. Montemor, *Rsc Advances*, 6 (2016) 15920.
21. H. Mu, C. Li, J. Bai and W. Sun, *Journal of Molecular Structure*, (2018) (in press).
22. E. Samuel, S. J. Hong, B. Joshi, S. An, H. G. Park, I. K. Yong, W. Y. Yoon and S. S. Yoon, *Electrochimica Acta*, 231 (2017) 582.
23. J. G. Wang, Y. Yang, Z. H. Huang and F. Kang, *Electrochimica Acta*, 170 (2015) 164.
24. S. Y. Kim, J. H. Wee, C. M. Yang and B. H. Kim, *Journal of Electroanalytical Chemistry*, (2017).
25. X. Feng, N. Chen, Y. Zhang, Z. Yan, X. Liu, Y. Ma, Q. Shen, L. Wang and W. Huang, *Journal of Materials Chemistry A*, 2 (2014) 9178.
26. E. Frackowiak and F. Béguin, *Carbon*, 39 (2001) 937.